

Spin-Density Distribution in $\text{CuCl}_2 \cdot 2\text{D}_2\text{O}^\dagger$

H. UMEBAYASHI,* B. C. FRAZER, D. E. COX, AND G. SHIRANE

Brookhaven National Laboratory, Upton, New York

(Received 6 November 1967)

The spin-density distribution in antiferromagnetic $\text{CuCl}_2 \cdot 2\text{D}_2\text{O}$ has been investigated at 1.7°K by neutron diffraction measurements. No appreciable concentrations of spin density were found except those localized about the Cu^{++} positions. The Fourier maps used in analyzing the neutron data did disclose a markedly aspherical distribution for the Cu^{++} spin density, however. A satisfactory explanation for the asphericity was obtained by consideration of the ground-state wave function of Cu^{++} in an orthorhombic crystalline field. The resulting wave function was found to consist of an admixture of two $d\gamma$ orbitals, about 90% ($x^2 - y^2$) and 10% ($3z^2 - r^2$). The neutron study also confirms the existence of a weak antiferromagnetic spin component, as predicted theoretically by Moriya. The form factor for this component is quite anomalous, however, indicating that it does not arise from a simple canting of the ionic moment.

I. INTRODUCTION

IN several respects, $\text{CuCl}_2 \cdot 2\text{H}_2\text{O}$ can be considered as typical of the ionic crystal antiferromagnets with low Néel temperatures. Since the crystal structure is relatively simple for this class of materials, one can hope to achieve an understanding of its magnetic properties in some detail. Consequently, this compound has been the subject of many investigations since the discovery of its antiferromagnetic phase below 4.3°K in the proton-magnetic-resonance experiments of Poullis and Hardeman.¹ These investigations have included further work with proton-magnetic-resonance data,^{2,3} Cl nuclear magnetic resonance,⁴ neutron diffraction measurements,^{5,6} and a number of theoretical studies.⁷⁻¹²

The present investigation was undertaken in an attempt to resolve two important questions which can best be answered through a detailed neutron diffraction study of a single-crystal specimen. In the first place, from the known proton positional parameters⁵ and the basic antiferromagnetic structure,^{1,6} the anisotropy of the proton-magnetic-resonance frequency cannot be explained on the basis of a simple dipole field from the Cu^{++} ions.² Calculations by Poullis *et al.*² of the internal field vector at the proton position indicated that the magnetic moment might be predominantly localized in

the region between the Cu^{++} and Cl^- ions. Although Cl NMR studies^{2,4} do not support this conclusion, it would be an important result if true, and it can be checked in a straightforward way by neutron diffraction. As described below, no appreciable concentrations of spin density were found in the present study except those localized normally about the Cu^{++} sites; however, a possible alternative explanation for the proton-resonance results is suggested.

The second question concerns the existence of a weak antiferromagnetic spin component which was predicted for this crystal by Moriya¹⁰ in his theoretical treatment of antisymmetric spin coupling. Although the basic antiferromagnetic spin structure has been determined,⁶ and indirect support for Moriya's canted arrangement has been suggested on the basis of transverse-susceptibility measurements,¹³ no direct experimental evidence for the latter had been reported until results were obtained in the present experiment. A preliminary account of these results has been reported briefly elsewhere.¹⁴

II. PRELIMINARY DETAILS

A. Experimental

Crystals of $\text{CuCl}_2 \cdot 2\text{D}_2\text{O}$ were grown by slowly cooling from 40°C a solution of CuCl_2 in 99.9% D_2O . The deuterated compound was chosen so as to avoid the large incoherent neutron scattering from hydrogen in the ordinary hydrate. As shown by Date,¹⁵ the magnetic properties of the hydrated and deuterated salts do not differ significantly.

A crystal having approximate dimensions of $3 \times 3 \times 6$ mm³, with its length along the a axis, was mounted with this axis parallel to the neutron-diffractometer axis. Diffraction measurements were carried out at the High Flux Beam Reactor at a neutron wavelength of 1.17₈ Å.

[†] Work performed under the auspices of the U.S. Atomic Energy Commission.

* Present address: Central Laboratory, Tohoku Metal, Yokohama, Japan.

¹ N. J. Poullis and G. E. G. Hardeman, *Physica* **18**, 201 (1952).

² N. J. Poullis, G. E. G. Hardeman, W. van der Lugt, and W. P. A. Hass, *Physica* **24**, 280 (1958).

³ R. E. Rundle, *J. Am. Chem. Soc.* **79**, 3372 (1957).

⁴ W. J. O'Sullivan, W. W. Simmons, and W. A. Robinson, *Phys. Rev.* **140**, A1759 (1965).

⁵ S. W. Peterson and H. A. Levy, *J. Chem. Phys.* **26**, 220 (1957).

⁶ G. Shirane, B. C. Frazer, and S. A. Friedberg, *Phys. Letters* **17**, 95 (1965).

⁷ T. Moriya and K. Yoshida, *Progr. Theoret. Phys. (Kyoto)* **9**, 663 (1953).

⁸ T. Nagamiya, K. Yoshida, and R. Kubo, *Advan. Phys.* **4**, Part I, 6 (1955).

⁹ W. Marshall, *J. Phys. Chem. Solids* **7**, 159 (1958).

¹⁰ T. Moriya, *Phys. Rev.* **120**, 91 (1960).

¹¹ R. J. Joenk, *Phys. Rev.* **126**, 565 (1962).

¹² A. C. Hewson, D. ter Haar, and M. E. Lines, *Phys. Rev.* **137**, A1465 (1965).

¹³ C. S. Naiman and T. R. Lawrence, *J. Appl. Phys.* **37**, 1138 (1966).

¹⁴ H. Umebayashi, G. Shirane, B. C. Frazer, and D. E. Cox, *J. Appl. Phys.* **38**, 1461 (1967).

¹⁵ M. Date, *J. Phys. Soc. Japan* **12**, 1168 (1957).

Data were collected at temperatures of 1.7 and 4.2°K. The aluminum sample container was charged with He gas for heat exchange before mounting in the cryostat, and was placed in direct contact with liquid He.

Since some of the magnetic peaks were very weak, especially those associated with the small canted spin component, elimination of half-wavelength contamination of the beam was essential. This was accomplished by employing the (113) plane of Ge for beam monochromatization. Other possible sources of systematic errors in the data considered were extinction effects and double-Bragg scattering. The magnetic intensities, even those associated with the principal magnetization component, are weak in comparison with the general level of observed nuclear intensities, and examination of the latter relative to calculated values showed that extinction effects were negligible at the low magnetic intensity levels. Double-Bragg scattering can only arise in the magnetic data by combinations of nuclear and

magnetic reflections. Because of the rapid falloff of the magnetic form factor, the number of combinations which could have an appreciable effect on the data is very limited. Therefore, even though the intensity data for the principal magnetic structure were not checked for double-Bragg reflection, it is unlikely that the data are contaminated significantly. Even a small contribution could be significant in the very-weak-intensity measurements associated with the small canted component, however, and checks were made in this case.

B. Crystallography

$\text{CuCl}_2 \cdot 2\text{D}_2\text{O}$ is crystallographically isomorphous with the ordinary hydrate. Structural data assumed in the present study were as follows: space group: orthorhombic Pbmn (D_{2h}^7); cell dimensions: $a=7.41 \pm 0.02$ Å, $b=8.08 \pm 0.02$ Å, $c=3.74 \pm 0.01$ Å; atomic coordinates:

2 Cu in 2(<i>a</i>):	$(0, 0, 0), (\frac{1}{2}, \frac{1}{2}, 0);$		
4 O in 4(<i>e</i>):	$\pm(0, y, 0), \pm(\frac{1}{2}, \frac{1}{2}+y, 0),$	$y=0.2390;$	
4 Cl in 4(<i>h</i>):	$\pm(x, 0, z), \pm(\frac{1}{2}-x, \frac{1}{2}, z),$	$x=0.2402,$	$z=0.3804;$
8 D in 8(<i>i</i>):	$\pm(x, y, z), \pm(\frac{1}{2}-x, \frac{1}{2}-y, z),$		
	$\pm(x, \bar{y}, z), \pm(\frac{1}{2}-x, \frac{1}{2}+y, z);$		
	$x=0.0822,$	$y=0.3065,$	$z=0.1295.$

The cell dimensions were measured at room temperature by x-ray diffraction using a small powdered specimen of the deuterated material. Corrections for minor changes in the cell because of cooling to low temperatures were made by experimental adjustments in the neutron-diffractometer settings. The coordinates listed are those determined by Peterson and Levy⁵ for the hydrate at room temperature. A least-squares analysis using a limited number of nuclear (*Ok**l*) structure factors observed at 4.2°K in the present study yielded a set of *y*- and *z*-coordinate parameters in close agreement with those listed above. The latter were therefore assumed unchanged in calculating intensities for scaling purposes.

A projection of the crystal structure with the canted spin structure proposed by Moriya¹⁰ superimposed is shown in Fig. 1. Two chemical unit cells are drawn in order to show the full magnetic cell.

III. SPIN-DENSITY DISTRIBUTION FOR MAJOR COMPONENT

A. Experimental Results

The basic antiferromagnetic structure of $\text{CuCl}_2 \cdot 2\text{H}_2\text{O}$ proposed originally by Poullis and Hardeman¹ was con-

firmed in a recent neutron diffraction study by Shirane *et al.*⁶ It is represented in Fig. 1 by the major components of the spin vectors, i.e., by the array of components parallel and antiparallel to the *a* direction. This structure gives rise to magnetic reflections with *h*+*k* even and *l* having a half-odd-integer value if the

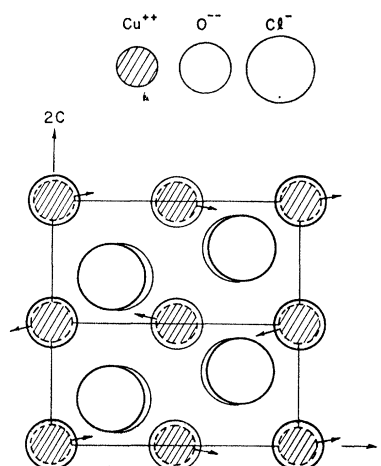


FIG. 1. The crystal structure of $\text{CuCl}_2 \cdot 2\text{D}_2\text{O}$ projected on (010). Arrows represent the moment directions as predicted by Moriya. Two chemical unit cells are shown.

reflecting plane is indexed on the chemical unit cell. Neutron-intensity data for 20 ($0k\frac{1}{2}l$) planes of this type, up to a $(\sin\theta)/\lambda$ value of 0.6, were collected in the present experiment on $\text{CuCl}_2 \cdot 2\text{D}_2\text{O}$. These data, reduced to yield an experimental magnetic form factor, are plotted as closed circles in Fig. 2. Normalization was based on agreement between the experimental and calculated intensities of the $(0, 0, \frac{1}{2})$ reflection.

As shown in Fig. 2, the experimental points deviate considerably from a smooth curve. Note also that the $(0, 0, \frac{1}{2}l)$ points fall off more slowly with angle than the other data. A Fourier spin-density projection, as shown in Fig. 3, disclosed that these irregularities in the experimental form factor are not due to a displaced spin distribution of the sort considered by Poulis *et al.*,² but rather to a pronounced asphericity in the localized spin density at the Cu^{++} site. A detailed examination of the computed numerical values for the Fourier map indicates that the additional spin density not associated with the Cu^{++} ion, if any, is less than 5% of that localized on the ion. Based on their Cl NMR measurements, O'Sullivan *et al.*⁴ gave a rough estimate of 0.1 for the fractional unpairing of the $3p$ Cl^- orbital. In view of the present results, this estimate seems to be on the high side.

An aspherical spin density for the Cu^{++} ion in an octahedral site is in accordance with the simple Jahn-Teller picture for the $3d^9$ configuration in which the degeneracy of the $d\gamma$ orbitals is removed by a tetragonal distortion ($c/a > 1$) with the unpaired electron in the $d_{x^2-y^2}$ orbital. The actual situation in $\text{CuCl}_2 \cdot 2\text{D}_2\text{O}$ is rather more complicated. The Cu^{++} ion is surrounded by two D_2O molecules, with each oxygen at a distance 1.92 Å from copper, and four Cl^- ions, two at 2.27 Å

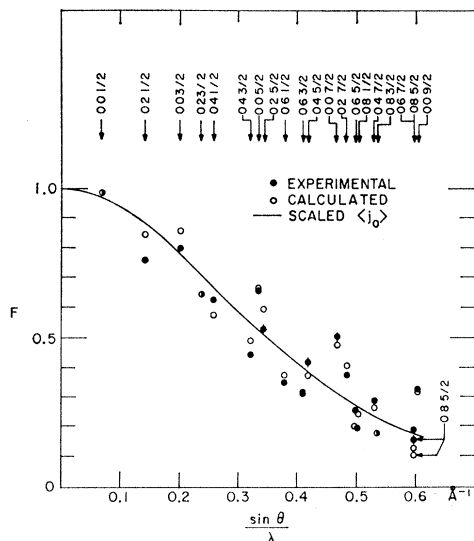


FIG. 2. Observed and calculated form factors for the main magnetic component in $\text{CuCl}_2 \cdot 2\text{D}_2\text{O}$. The calculated values and the scaled values of $\langle j_0 \rangle$ were obtained with the parameters $\alpha=0.1$ and $\beta=0.93$, as described in the text.

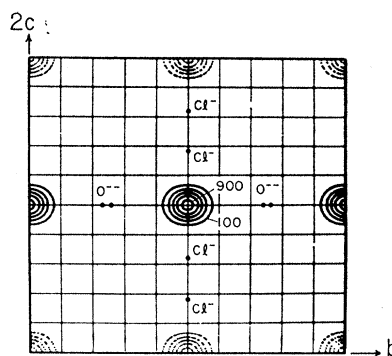


FIG. 3. Spin density projected onto (100). Density contours are drawn at intervals of 200, with a scaled peak value of 1000 units. Broken contours represent regions of negative spin density. The projected locations of the Cl^- and O^- ions are also shown.

and two at 2.91 Å. The latter pair define the long z axis of the distorted octahedron. The over-all symmetry of the ligand crystalline field is orthorhombic to a very good approximation, and the three principal axes are chosen as indicated in Fig. 4. The η axis is parallel to the crystallographic b axis and is common to the corner and base-center Cu^{++} ions, while the ξ and ζ axes are tilted 37.6° and 38.6° from the a and c axes, respectively. It will be assumed that both the ξ and ζ axes are tilted by 38° in the calculations which follow.

B. Form-Factor Calculations

The ground-state wave function of a Cu^{++} ion, which has a single hole in its $3d$ orbitals, in an orthorhombic crystalline field has been discussed by Moriya and Yoshida⁷ in their calculation of the magnetic anisotropy of this material. It is written as an admixture of two $d\gamma$ orbitals;

$$\psi_0 = (1 + \alpha^2)^{-1/2} [\frac{1}{2}\sqrt{2}(12) + 1(-2) + \alpha 10], \quad (1)$$

where 1 ± 2 and 10 are the free-ion wave functions with $m = \pm 2$ and 0 , respectively; the quantization axis is taken as the ζ axis, and α is the real admixture parameter, which depends upon how strongly orthorhombic the crystalline field is ($\alpha=0$ for a tetragonal field). The first term in (1) is one of the two $d\gamma$ orbitals of the form $\xi^2 - \eta^2$, whose density contours are shown schematically in Fig. 4, and the last term is the other $d\gamma$ orbital of the form $3\zeta^2 - \rho^2$, where ρ is the position vector (ξ, η, ζ) .

The aspherical form factor f of a transition-metal ion in a crystalline environment may be calculated following the procedure of Weiss and Freeman¹⁶:

$$f = \int \psi_0^* \exp(-i\mathbf{k} \cdot \boldsymbol{\rho}) \psi_0 d\boldsymbol{\rho}, \quad (2)$$

where \mathbf{k} is the scattering vector. This integral can be evaluated by using the tables given by Weiss and

¹⁶ R. J. Weiss and A. J. Freeman, J. Phys. Chem. Solids 10, 147 (1959).

Freeman,¹⁶ with the result that

$$f = \langle j_0 \rangle + \left[\frac{1-\alpha^2}{1+\alpha^2} \frac{5}{7} (3 \cos^2\theta - 1) + \frac{2\alpha}{1+\alpha^2} \frac{5\sqrt{3}}{7} \cos 2\phi \sin^2\theta \right] \langle j_2 \rangle + \left[\frac{1+6\alpha^2}{1+\alpha^2} \frac{3}{56} (3 - 30 \cos^2\theta + 35 \cos^4\theta) - \frac{2\alpha}{1+\alpha^2} \frac{15\sqrt{3}}{28} \cos 2\phi (1 - 8 \cos^2\theta + 7 \cos^4\theta) + \frac{1}{1+\alpha^2} \frac{15}{8} \cos 4\phi \sin^4\theta \right] \langle j_4 \rangle, \quad (3)$$

where θ and ϕ are the polar angles of the scattering vector \mathbf{k} in the (ξ, η, ζ) coordinate system, and $\langle j_0 \rangle$, $\langle j_2 \rangle$, and $\langle j_4 \rangle$ are functions of $|k|$ as defined in Ref. 16. Numerical values of the latter have been tabulated by Watson and Freeman¹⁷ for various $3d$ elements and ions.

Generally speaking, (3) gives different values for magnetic ions whose coordination axes are differently oriented, e.g., for the corner and base-center Cu^{++} ions in this crystal. In the present experiment, however, the scattering vectors always lie in the (100) plane, and the coordinate systems for the corner and base ions are related by mirror reflection parallel to this plane. Therefore $\cos^2\theta$ and $\cos 2\phi$, and accordingly f , have the same values in each case.

In calculations carried out over a range of α values, good agreement with the general behavior of the experimental points in Fig. 2 was obtained for a value of $\alpha \approx 0.1$. However, a systematic discrepancy was still evident between the experimental and calculated values, in that the former had higher values than the latter at high angles. An additional phenomenological parameter β was introduced to improve the agreement, by expanding the spherical part of the form factor as done by Alperin¹⁸ in his calculation for NiO, such that the scaled form factor $f_s(x) = \langle j_0 \rangle(\beta x)$, where $x = (\sin\theta)/\lambda$. The best fit was obtained by choosing $\beta = 0.93$, resulting in an improvement of 15% in the standard deviation compared to the calculation with $\beta = 1$. The calculated form factors for $\alpha = 0.1$ and $\beta = 0.93$ are shown in Fig. 2 by the open circles, together with the scaled spherical form-factor curve f_s . The over-all agreement with the experimental points is satisfactory, although there are still some unexplained discrepancies in the low-angle reflections.

The admixture parameter α can also be estimated from the anisotropy of the g factors, since it may be expressed as follows⁷:

$$g_{\xi} - g_{\eta} = -8\sqrt{3}\alpha\gamma/(1+\alpha^2), \quad (4)$$

where it is assumed that the orthorhombic energy splitting between the two highest $d\epsilon$ orbitals $|1\rangle \pm |-1\rangle$ is much smaller than the cubic energy separation, and

¹⁷ R. E. Watson and A. J. Freeman, *Acta Cryst.* **14**, 27 (1961); and (private communication).

¹⁸ H. A. Alperin, *Phys. Rev. Letters* **6**, 55 (1961).

that the ratio γ of the spin-orbit coupling coefficient λ to the energy separations from the ground state for the two excited states is the same in each case. Taking $\gamma = -0.032$,¹⁹ and $g_{\xi} - g_{\eta} = 0.036$,²⁰ then $\alpha \approx 0.08$, which is in good agreement with the value of 0.1 found above.

The value of $\beta = 0.93$ obtained in expanding the spherical part of the Cu^{++} form factor means that the spin density is *contracted* by 7% in its crystalline environment in this compound, as compared to the free-ion spin density predicted by Watson and Freeman.¹⁷ The reason for this is not clear, although spin polarization of the otherwise "paired" orbitals,²¹ an orbital-moment contribution to the form factor,²² and a covalency effect²³ have all been invoked to explain the similar observation of Alperin¹⁸ in NiO.

C. Interpretation of the Resonance Data

Since with the accuracy limits of the present experiment the spin density has been shown to be localized at

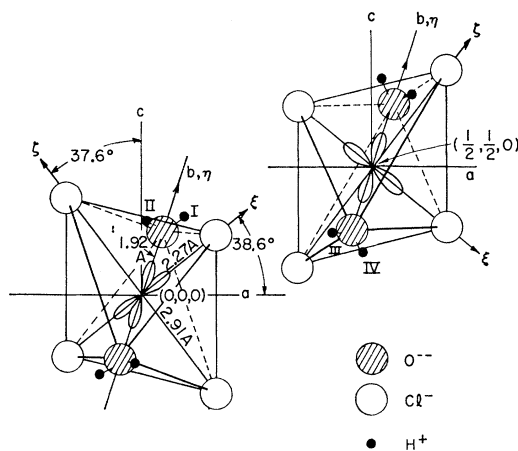


FIG. 4. Crystal-structure environment of the corner and base-center Cu^{++} ions. The schematic electron-density contour of the ground-state orbitals and the coordinate system used in the calculation are also shown.

¹⁹ D. Polder, *Physica* **9**, 709 (1942).

²⁰ J. Itoh, M. Fujimoto, and H. Ibamoto, *Phys. Rev.* **83**, 852 (1951).

²¹ A. J. Freeman and R. E. Watson, *Phys. Rev.* **120**, 1125 (1960).

²² M. Blume, *Phys. Rev.* **124**, 96 (1961).

²³ J. Hubbard and W. Marshall, *Proc. Phys. Soc. (London)* **86**, 561 (1956).

the Cu^{++} sites, it is of interest to consider the bearing of this result on an interpretation of the proton-resonance data.² First, one might examine the possibility of explaining the resonance results in terms of the strong asphericity in the Cu^{++} spin distribution. This was tested by computing the dipole field at a proton position in a summation over fifty nearest-neighbor Cu^{++} ions. The effects due to asphericity were taken into account approximately by splitting the ionic moment into four-point dipoles, displaced at a distance of about 0.4 Å along the bond directions shown in Fig. 4, for the five first nearest neighbors. This aspherical refinement resulted in very little change in the dipole-field components. Absolute values obtained for the components were $H_x=30$ Oe, $H_y=450$ Oe, and $H_z=30$ Oe, as compared to experimental values of $H_x=539$ Oe, $H_y=378$ Oe, and $H_z=380$ Oe. The origin of the internal field must therefore be sought for elsewhere.

An investigation was made into the effects of unpaired charge transfers of magnitudes too small to be detected in the neutron diffraction experiment. One possible mechanism was found which could play an important role in accounting for the internal field. A transfer of a very small fraction of an unpaired electron from a Cu^{++} ion to a nearest-neighbor water molecule can produce effects of about the right order of magnitude. For example, if a moment of only $0.02\mu_B$ is assumed at an O^{--} site, a dipole field of about 300 Oe is produced at a proton position. Moreover, one can expect an internal field of about 600 Oe, parallel or antiparallel to the Cu^{++} moment, through the Fermi contact interaction when the $1s$ orbitals of the water-molecule hydrogens have a net unpaired electron spin of $0.002\mu_B$ (estimated²⁴ from the hydrogenic $1s$ wave function with a screened charge $Z=1.2$). For a quantitative treatment, a much more detailed knowledge of the bonding character of the crystalline water is clearly required.

IV. CANTED SPIN STRUCTURE

From symmetry considerations, an antisymmetric superexchange interaction of the type $\mathbf{D}_{12} \cdot (\mathbf{S}_1 \times \mathbf{S}_2)$

TABLE I. Observed integrated intensities corrected for angle factor of the minor magnetic peaks in $\text{CuCl}_2 \cdot 2\text{D}_2\text{O}$. φ is the angle between the reflecting plane and the spin axis [001].

hkl	Relative intensity	φ
$0, 1, \frac{1}{2}$	137 ± 30	47.2°
$0, 3, \frac{3}{2}$	235 ± 80	19.8°
$0, 1, \frac{3}{2}$	348 ± 30	72.0°
$0, 3, \frac{5}{2}$	324 ± 50	47.2°
$0, 5, \frac{1}{2}$	115 ± 60	12.2°

²⁴ R. E. Watson (private communication).

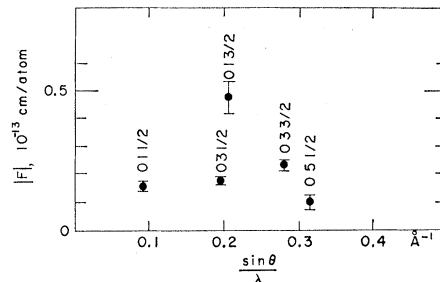


FIG. 5. Experimental magnetic form factor of the minor spin component. Error bars were estimated from a combination of statistical errors and differences in intensity from equivalent reflections in different quadrants.

between two Cu^{++} spins should lead to a minor spin component parallel to the c axis in $\text{CuCl}_2 \cdot 2\text{D}_2\text{O}$ if a four-sublattice model is assumed.¹⁰ The minor components form an antiferromagnetic array with a different configurational symmetry from that of the basic magnetic structure obtained from the major spin component. The expected canted spin structure is shown in Fig. 1.

Neutron-reflection conditions for the minor-component structure are $h+k$ odd and l equal to a half-odd integer, and hence the diffraction data are completely independent of the major spin component. Although the neutron intensities are very weak, the five most favorable reflections were observed in the present experiment. The peak-to-background ratio was about 1:6 in the worst case. The observed integrated intensities, with the $\sin 2\theta$ factor removed, are listed in Table I. The error limits in the table were estimated from a comparison of data from equivalent quadrants, as well as from counting statistics. If the intensity data are processed on the basis of Moriya's predicted model, a magnetic form factor is obtained for the minor spin component as shown in Fig. 5.

Since these data are derived from very-weak-intensity observations, and the form factor has an unusual shape, the question must be considered as to whether they represent valid measurements for the minor spin component. The following points are pertinent:

(1) Systematic errors in measurements. Since the neutron beam was free of $\frac{1}{2}\lambda$ contamination, the only significant measurement errors that could arise would be from double-Bragg scattering. Because of the doubled magnetic cell, the latter could only result from combinations of nuclear and magnetic reflections. Experimental checks were made for this for the $(0, 1, \frac{1}{2})$ and $(0, 1, \frac{3}{2})$ reflections by rotating the crystal about the scattering vector over a range of several degrees in each direction from the vertical a -axis setting. No appreciable changes in intensity were detected, and therefore any double-Bragg contributions were negligibly small.

(2) Crystallographic phase change. The weak peaks disappeared on warming the crystal to the Néel point. Also, no intensity changes were observed in the nuclear peaks on passing through the Néel point. These checks strongly indicate that the weak peaks are truly magnetic in origin, although the possibility of some small change in the crystal structure cannot be ruled out absolutely.

(3) Extended spin density of major component. One question to consider is whether the aspherical major-component spin density of the Cu^{++} ions, or some collinear unpaired charge associated with the anions, could give rise to otherwise forbidden peaks. The extinction rules for the case of nonzero spin density in general positions and oriented parallel to the a axis are, however, the same as those for the Cu^{++} special positions. The magnetic symmetry requires, in fact, that the weak peaks can only result from a spin-density distribution oriented parallel to the c axis.

From the above considerations, we conclude that the data confirm the existence of a small canted spin-density component as predicted by Moriya.¹⁰ The data are too few to confirm his model in detail, as will be considered further below. However, if Moriya's model is assumed, the form factor in Fig. 5 is reasonably consistent with his predicted value of $0.1\mu_B$ for the minor-spin-component magnitude.

From the unusual shape of the form factor, it is clear that the spin density associated with the minor component is quite different from that of the major component. This was also observed in the case of $\alpha\text{-Fe}_2\text{O}_3$ by Nathans *et al.*,²⁵ and has been examined theoretically for that crystal by Kaplan.²⁶ Nathans *et al.* were able to account for their observations on the basis of a simplified displaced-charge model, but because of the small number of data, they were careful to point out that their interpretation was not necessarily unique. The situation with $\text{CuCl}_2 \cdot 2\text{D}_2\text{O}$ is very similar. Reasonably good agreement between calculated and observed intensities can be obtained, for example, by placing roughly equal unpaired charges on the Cu^{++} and Cl^- , with the Cl^- charge directed opposite to its nearest Cu^{++} neighbor, but this is probably only one of several models capable of fitting the data. As in the case of $\alpha\text{-Fe}_2\text{O}_3$, the important conclusion to be drawn is that the Moriya component does not arise from a simple

canting of the Cu^{++} ionic moment, but rather the magnetization density must be considered as a vector function of position in the unit cell.

V. CONCLUDING REMARKS

The neutron diffraction measurements reported here establish that the spin density associated with the basic antiferromagnetic structure of $\text{CuCl}_2 \cdot 2\text{D}_2\text{O}$ is well localized on the Cu^{++} ions, and that the observed asphericity of this density can be explained by consideration of the ground-state orbital of Cu^{++} in an orthorhombic crystalline field. Any spin density elsewhere in the structure cannot exceed a level of about $0.05\mu_B$ in its component parallel to the major component of the Cu^{++} ionic moment. Arguments involving a substantial concentration of unpaired charge on or near the Cl^- ions are therefore invalid, and an explanation of the results of proton-resonance studies^{2,3} must be based on a different mechanism. Nor does it seem possible to account for the field at the proton positions in terms of the marked asphericity in Cu^{++} spin distribution observed in the present investigation. On the other hand, it does seem possible, qualitatively at least, to obtain a field of about the proper intensity by assuming a very small amount of unpaired charge on the water molecules. The magnetization density for this charge is much too small to be detected in an unpolarized neutron diffraction experiment, however.

The neutron data also confirm the existence of a weak antiferromagnetic spin component perpendicular to that of the basic structure, in agreement with the theoretical prediction of Moriya.¹⁰ The measurements were insufficient in number to analyze the spin-density distribution for this component, but it is evident from the angular dependence of the data that the distribution is quite different from that associated with the main component of the ionic moment. It is difficult to say how the data in Fig. 5 should be extrapolated to zero scattering angle to yield an effective moment, but the value of $0.1\mu_B$ predicted by Moriya is not unreasonable.

ACKNOWLEDGMENTS

The authors would like to thank M. Blume, S. A. Friedberg, F. Menzinger, V. J. Minkiewicz, R. Nathans, R. E. Watson, and W. R. Wright for their valuable suggestions and many helpful discussions. They also wish to thank F. Merkert for his able assistance in growing the sample crystal.

²⁵ R. Nathans, S. J. Pickart, H. A. Alperin, and P. J. Brown, *Phys. Rev.* **136**, A1641 (1964).

²⁶ T. A. Kaplan, *Phys. Rev.* **136**, A1636 (1964).